Possible association of the western Tibetan Plateau snow cover with the decadal to interdecadal variations of northern China heatwave frequency

Zhiwei Wu, Zhihong Jiang, Jianping Li, Shanshan Zhong & Lijuan Wang

Climate Dynamics
Observational, Theoretical and Computational Research on the Climate System

ISSN 0930-7575
Volume 39
Combined 9-10

Clim Dyn (2012) 39:2393-2402
DOI 10.1007/s00382-012-1439-4

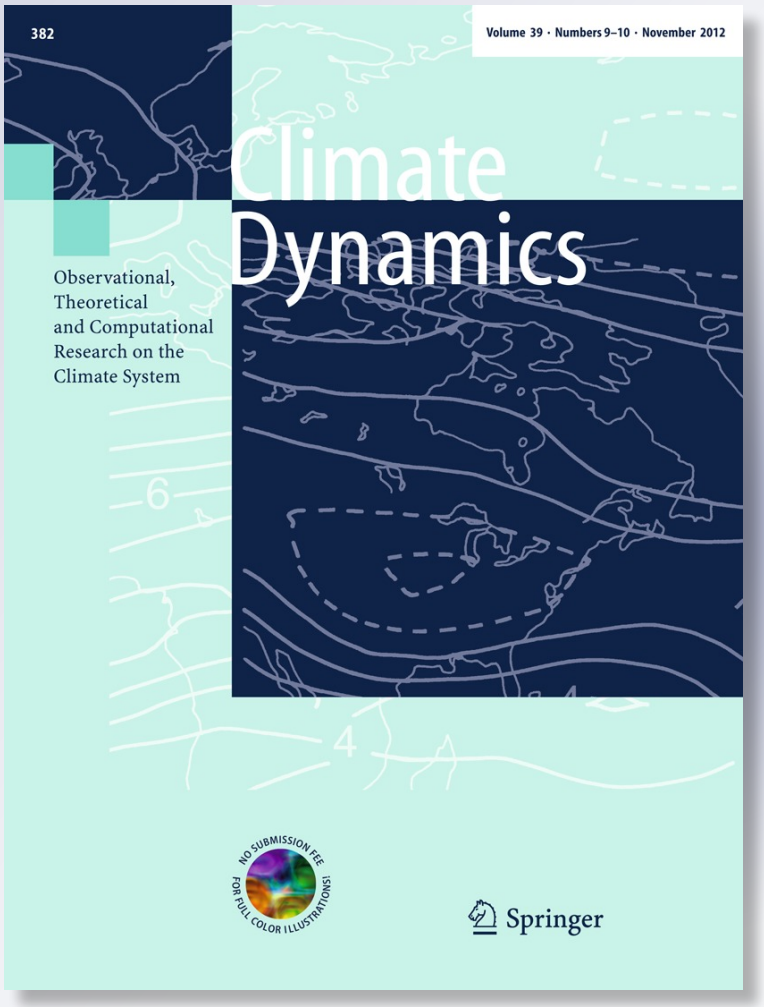

Springer

Clim Dyn (2012) 39:2393–2402
DOI 10.1007/s00382-012-1439-4

ORIGINAL ARTICLE

Possible association of the western Tibetan Plateau snow cover with the decadal to interdecadal variations of northern China heatwave frequency

Zhiwei Wu · Zhihong Jiang · Jianping Li · Shanshan Zhong · Lijuan Wang

Received: 16 August 2011 / Accepted: 26 June 2012 / Published online: 11 July 2012

Abstract Northern China has been subject to increased heatwave frequency (HWF) in recent decades, which deteriorates the local droughts and desertification. More than half a billion people face drinking water shortages and worsening ecological environment. In this study, the variability in the western Tibetan Plateau snow cover (TPSC) is observed to have an intimate linkage with the first empirical orthogonal function mode of the summer HWF across China. This distinct leading mode is dominated by the decadal to inter-decadal variability and features a mono-sign pattern with the extreme value center prevailing over northern China and high pressure anomalies at mid- and upper troposphere over Mongolia and the adjacent regions. A simplified general circulation model is utilized to examine the possible physical mechanism. A reduced TPSC anomaly can induce a positive geopotential height anomaly at the mid- and upper troposphere and subsequently enhance the climatological high pressure ridge over Mongolia and the adjacent regions. The subsidence associated with the high pressure anomalies tends to suppress the local cloud formation, which increases the net radiation budget, heats the surface, and favors more heatwaves. On the other hand, the surface heating can excite high pressure anomalies at mid- and upper troposphere. The latter further strengthens the upper troposphere high pressure anomalies over Mongolia and the adjacent regions. Through such positive feedback effect, the TPSC is tied to the interdecadal variations of the northern China HWF.

Keywords Tibetan Plateau snow cover · Heatwave · Decadal to interdecadal variations

Z. Wu (✉) · Z. Jiang · S. Zhong · L. Wang
Key Laboratory of Meteorological Disaster of Ministry of Education, Nanjing University of Information Science and Technology, Nanjing, China
e-mail: wzw.lasg@gmail.com; zhiweiwu@hawaii.edu

Z. Wu · J. Li
State Key Laboratory of Numerical Modeling for Atmospheric Sciences and Geophysical Fluid Dynamics, Institute of Atmospheric Physics, Chinese Academy of Sciences, Beijing, China

1 Introduction

Under the global warming background, heatwaves have become a major meteorological disaster on the Earth (Trenberth et al. 2007). For example, over 25,000 deaths were attributable to the 2003 heatwave in Europe (Garcia-Herrera et al. 2010). In the summer of 2010, Moscow experienced 33 consecutive days with maximum temperatures exceeding 30 °C. This unprecedented heatwave took 15,000 lives and cost the economy $15 billion as fires and drought ravaged the country (Alexander 2010).

Northern China has also undergone frequent heatwaves, associated with a severe drought and desertification trend during summer in the past decades (e.g., Zhai et al. 1999; Fu 2003; Wang and Ding 2006; Trenberth et al. 2007; Ding et al. 2007). More than half a billion people are facing drinking water shortages, which triggers the South-North Water Transfer Project to better utilize water resources available to China (http://www.nsbd.gov.cn/). Therefore, understanding the origins of the northern China heatwaves is obviously of great societal as well as scientific values. This motivates the present study.

The reasons for the northern China heatwaves are far from being clarified. Most of the previous studies primarily focus on the northern China rainfall variations rather than

the heatwaves. For example, Fu (2003) proposed that the human-induced land cover change may impact on the northern China drought tendency. Based on the observational and theoretical evidences, Li et al. (2010) suggested that the regionally meridional asymmetric warming with the most prominent surface warming center in northeastern Asia can induce the southward shift of the Meiyu–Baiu–Changma rain belt and in turn lead to the droughts over northern China.

The reason why the northern rainfall receives more research interests than surface air temperature is partly due to the fact that the rainfall has a more direct impact on the local droughts and partly due to the assumption that surface air temperature usually exhibits coherent variations with rainfall. However, the relationship between the summer precipitation and surface air temperature is rather complicated. For instance, in the eastern China, significant negative correlations between summer precipitation and air temperature are mainly along the middle and lower reaches of the Yangtze River valley, while the correlations may be less significant in other regions (Nitta and Hu 1996). Hirschi et al. (2010) used observations of surface air temperature and precipitation in Europe and found that soil-moisture deficits are likely to have enhanced the frequency and duration of extreme summer heat in southeastern Europe. However, they also noted that for wetter climates, such as that in central Europe, observations indicate only a weak relationship between heatwaves and precipitation variations.

Northern China is dominated by transitional climate from monsoon to desert (e.g., Ding 1992). The subtropical front of the East Asian summer monsoon can bring notable precipitation to northern China in some strong monsoon years, and vice versa in some weak monsoon years (e.g., Wang et al. 2008b; Wu et al. 2009). The coupling between the heatwave and precipitation is of considerable year-to-year differences in this region. Therefore, it is necessary to re-investigate the heatwave origins over northern China, in spite that many studies have been conducted on the local rainfall variations. In this study, we focus on the potential association of the Tibetan Plateau (TP) snow cover (TPSC) with the heatwave frequency (HWF) over China.

The TPSC anomalies were found to have a close connection with the Asian climate, especially the East Asian summer monsoon (e.g., Qian et al. 2003; Yu et al. 2004; Massimo and Benedict 2004; Zhang et al. 2004; Li et al. 2005; Wu et al. 2007; Wu and Kirtman 2007; Zhao et al. 2007; Wang et al. 2008a; Seol and Hong 2009; Duan et al. 2011; Liu and Chen 2011; Wu et al. 2012; and many others). With the highest mountains in the world, the TPSC can persist through the warm seasons over the high-altitude areas (Pu et al. 2007; Wu et al. 2012), making it a potential predictability source for summer climate. During summer (June–August, JJA), the most persistent snow cover is located in the western and southern TP within large mountain ridges.

In this paper, we attempt to answer whether and how the TPSC is connected with the HWF variability across China. Section 2 describes the datasets, model and methodology used in this study. Section 3 presents the observed relationship between the TPSC and the China HWF. In Sect. 4, numerical experiments are carried out with a simple general circulation model (SGCM) and the possible physical mechanism is explored. The last section summarizes major findings and some outstanding issues.

2 Data, model and methodology

The major datasets used in this work include: (1) daily surface air temperature data at 605 gauge stations across China from China Meteorological Administration (see black dots in Fig. 1); (2) 1968–2009 monthly snow cover area extent data from the Global Snow Lab (Rutgers University) (http://climate.rutgers.edu/snowcover/); (3) the monthly circulation data, gridded at 2.5° × 2.5° resolution, taken from the European Centre for Medium-Range Weather Forecasts (ECMWF) 40-year reanalysis dataset (ERA-40; Uppala et al. 2005) and the ERA-interim dataset; (4) the monthly total cloud cover (TCC) and the surface solar radiation data (SSR) obtained from the ECMWF. Note that the ERA-40 data are extended from 2003 to 2009 by using ERA-interim data. To maintain temporal homogeneity, the 2003–2009 ERA-interim data are adjusted by removing the climatological difference between the ERA-40 and ERA-interim data (see the method in Wang et al. 2010).

The numerical experiments are based on the SGCM as described in detail in Hall (2000). The resolution used here is triangular 31, with 10 equally spaced sigma levels as in Wu et al. (2009). We used the National Centers for Environmental Prediction (NCEP) reanalysis version 1 (NCEP-1; Kalnay et al. 1996) data to drive the numerical experiments. An important feature of this model is that it uses a time-averaged forcing calculated empirically from observed daily data. As shown in Hall (2000), this model is able to reproduce remarkably realistic stationary planetary waves and the broad climatological characteristics of the transients are in general agreement with the observations.

According to the definition by Fischer and Schär (2010), a heatwave is defined as a spell of at least six consecutive days with maximum temperatures exceeding the local 90th percentile of the control period (1961–1990). To account for the seasonal cycle, the 90th percentile is calculated for each calendar day, and at each grid point using a centered 15-day-long time window. The HWF refers to the average

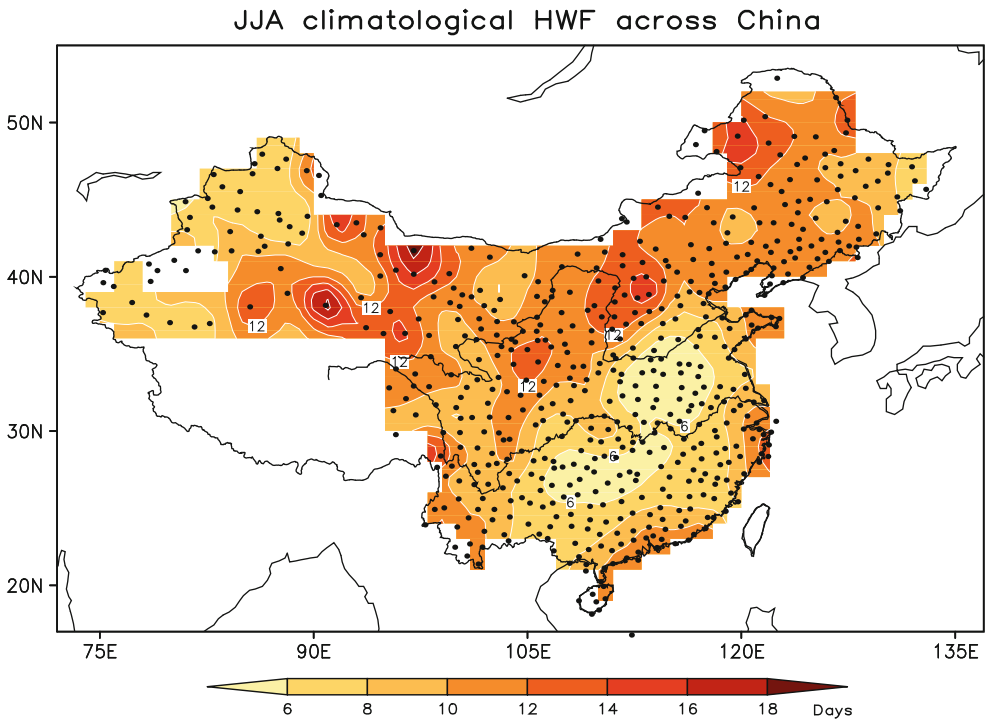

Fig. 1 The climatological heatwave frequency (HWF) across China for June–August (JJA) (*color shadings* in unit of day). *Black dots* denote 605 surface air temperature (SAT) gauge stations across China

frequency of days meeting the heatwave criterion. To derive the leading modes of the HWF, we performed an Empirical Orthogonal Function (EOF) analysis by constructing an area-weighted covariance matrix.

The major snow cover areas in summer are basically located in the western and southern Plateau regions (particularly the Himalaya Mountains), which have higher altitudes and therefore, are favorable for the snow cover persisting through summer. Most of the interior of the Plateau with lower altitudes has relatively less snow cover persistence (Pu et al. 2007; Wu et al. 2012). To quantitatively measure the TPSC variations, we used a TPSC index (TPSI) proposed by Wu et al. (2012). This index is defined as the snow cover averaged within the domain (70°–80°E, 31°–41°N) where the summer climatology center and the year-to-year variability maximum are located (see Fig. 1 in Wu et al. 2012). Such notable snow cover changes yield significant low boundary forcing signals for the atmosphere (e.g., Wang et al. 2008a; Wu et al. 2012).

3 The China HWF and TPSC

Figure 1 presents the climatology of the JJA HWF across China. A prominent feature is that the HWF values in northern China are generally larger than those in southern China, with the maximum in northwestern China, the desert region. Since most areas in northern China belong to dry or semi-dry regions, such pattern indicates that heatwaves are more frequent to occur in dry regions than in wet regions. This is consistent with the notion of extreme heat rooted in dry soils (e.g., Alexander 2010; Hirschi et al. 2010).

Figure 2 displays the two leading EOF modes of the HWF across China. The first mode accounts for 27.3 % of the total variance, and the second mode 12.5 % (Fig. 2a and c). According to the rule given by North et al. (1982), the two leading modes are statistically distinguished from each other. They are also separable from the rest of the other high modes in terms of the sampling error bars (not shown). The EOF1 mode basically bears a mono-sign pattern with maximum loading located in northern China and therefore, is labeled as the northern China mode, its amplitude decreasing southward (Fig. 2a). PC1 is primarily dominated by an interdecadal increasing trend with significant interannual variations superposed upon it (Fig. 2b). Most of the years before mid-1990s have a negative PC1, while those after mid-1990s a positive PC1. A positive PC1 refers to more heatwaves over northern China, and vice versa. Therefore, the EOF1 mode reflects the interdecadal increase in northern China HWF. This result is consistent with the observed fact that the most severe warming over eastern Asia takes place in northern China and the interdecadal shift of China summer climate in 1996–1998 (Hu 1997; Trenberth et al. 2007; Li et al. 2010; R. Wu et al. 2010).

The prominent feature of the EOF2 mode is a meridional dipole pattern with anomalies of opposite signs

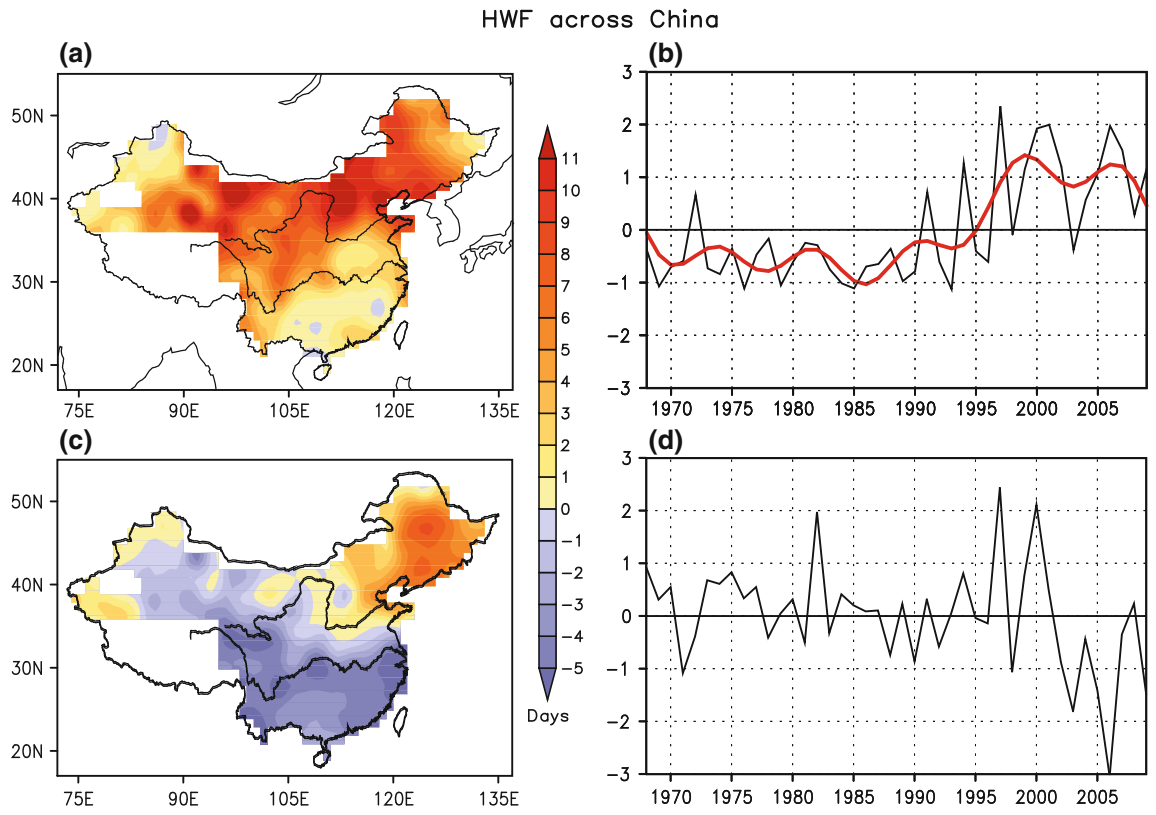

Fig. 2 *Upper panels*: **a** spatial pattern (*color shadings* in unit of day) and **b** the corresponding principal component (PC) of the first empirical orthogonal function (EOF) mode of the JJA HWF across China. *Lower panels* **c** and **d**: same as in **a** and **b** but for the second mode. The numbers in the brackets indicate fractional variance of the EOF modes. The *red curve* in **b** is the decadal-to-interdecadal component (ID) of PC1, namely, PC1(ID)

between the northern and southern China (Fig. 2c). The extreme value center is located in northeastern China. A high PC2 year is corresponding to a more HWF in northern China and less in southern China, and vice versa. The amplitude of PC2 has considerably amplified since mid-1990s (Fig. 2d), suggesting that the EOF2 pattern become more obvious after mid-1990s. Moreover, the EOF2 pattern highly resembles the anomalous summer precipitation pattern over China (e.g., Zhu et al. 2007), indicating a coupled linkage between the HWF and the local rainfall.

It is interesting to notice that the TPSC exhibits an intimate linkage with the northern China mode (Fig. 3). In corresponding to the increasing tendency of PC1 (red curve in Fig. 2b), the TPSI displays a decreasing trend after mid-1990s, indicating a reduced TPSC (Fig. 3a). To focus on the decadal-to-interdecadal (ID) time scales, PC1 and TSPI has been smoothed through keeping all Fourier harmonics that have periods longer than 8 years and labeled as PC1(ID) and TPSI(ID), respectively (red curves in Figs. 2b, 3a). The HWF pattern that is projected as a result of the decreasing TSPC resembles to the EOF1 mode (Figs. 2b, 3b), namely, featuring an extreme center over northern China. In light of the close connection between the TPSC and northern China mode, this study will focus on how the more slowly involving TPSC decreasing modulates the northern China HWF.

Before investigating the physical mechanism, we need to clarify the planetary-scale three-dimensional circulation structure associated with the northern China mode and the anomalous TPSC, respectively. In general, the large-scale circulation anomalies regressed against PC1(ID) resemble a similar pattern with that against TPSI(ID) (Figs. 4, 5, 6). Near the surface (Fig. 4b, c), a large area of positive sea level pressure (SLP) anomalies occupies the northern China with a major ridge extending southwestward towards TP. Comparing with the climatology, this pattern reflects the high pressure anomalies over Mongolia and the adjacent regions. Such feature is more evident at the middle and upper troposphere (Figs. 5, 6). The enhanced high accompanied by anti-cyclonic wind anomalies prevails over northern China, with the high ridge axis tilting toward TP (Figs. 5c, 6c). Such high ridge tilting implies its linkage with the TPSC, which is consistent with the results by Zhao et al. (2010). In addition, weak negative geopotential height anomalies (GHAs) and cyclonic wind anomalies prevail over South China.

To verify whether the above high pressure anomalies over Mongolia and the adjacent regions can also be

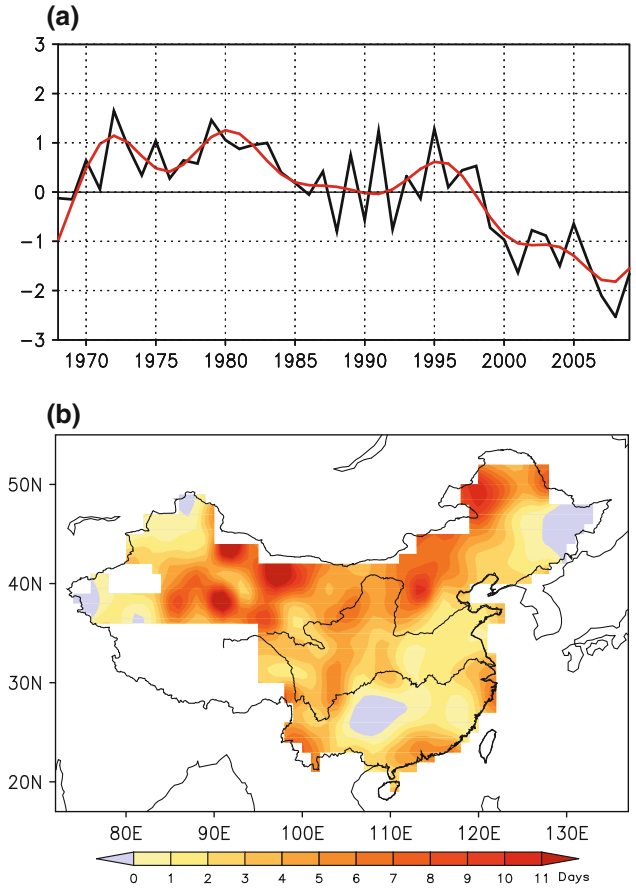

Fig. 3 **a** Time series of the normalized Tibetan Plateau (TP) snow cover index (TPSI) (*black curve*) and its decadal-to-interdecadal component TPSI(ID) (*red curve*) for the 1968–2009 summers (JJA); **b** The JJA HWF anomalies regressed to the TPSI(ID) (*color shadings* in unit of day). For comparison purpose, the sign of the TPSI(ID) time series has been reversed, hereafter

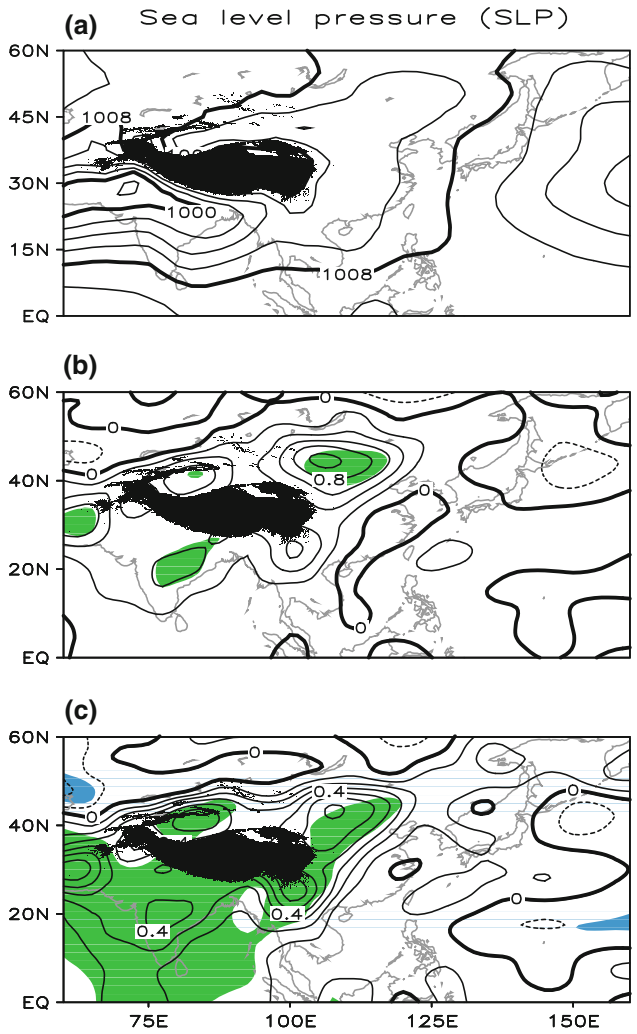

Fig. 4 **a** JJA climatology in sea level pressure (SLP; contours in unit of hPa) and their anomalies regressed to the **b** PC1(ID) and **c** TPSI(ID). The *black shadings* denote TP, and the *color shadings* the 95 % confidence level based on the Student's *t* test

observed in anomalous TPSC summers, we calculate the composite difference of circulations between the reduced and excessive TPSC decades (Fig. 7). According to the evolution feature of TPSI(ID) (Fig. 3a) and some previous studies (Yu et al. 2004; Sutton and Hodson 2005; Zhao et al. 2010), the 1972–1995 and 1996–2009 periods are defined as the reduced and excessive TPSC decades, respectively. It can be clearly seen from Fig. 7 that the high pressure anomalies over Mongolia and the adjacent regions are evident over the mid- and upper troposphere, 500 hPa in particular. A salient high pressure center controls northern China and expands towards TP. The vertical high ridge also tilts towards TP. A weak low anomaly covers South China. These high pressure anomalies over Mongolia and the adjacent regions are considerably similar to those accompanied by the northern China mode.

From the above statistical analysis, the linkage among the northern China HWF, the high pressure anomalies over Mongolia and the adjacent regions and the TPSC may be summarized as following: the northern China HWF anomalies are usually associated with the GHAs over Mongolia and the adjacent regions, while the GHAs are significantly related to the TPSC variations. However, the correlations do not warrant any cause and effect.

4 Physical mechanisms

How can the TPSC affect the HWF over northern China? To figure out this question, we need to understand how the atmospheric anomalies over Mongolia and the adjacent regions couple with the HWF anomalies over northern China. Then, it should be answered whether and how the TPSC influences the atmospheric anomalies over Mongolia and the adjacent regions.

We take PC1(ID) as a reference and compute the lead-lag regression with 200 hPa geopotential height (H200)

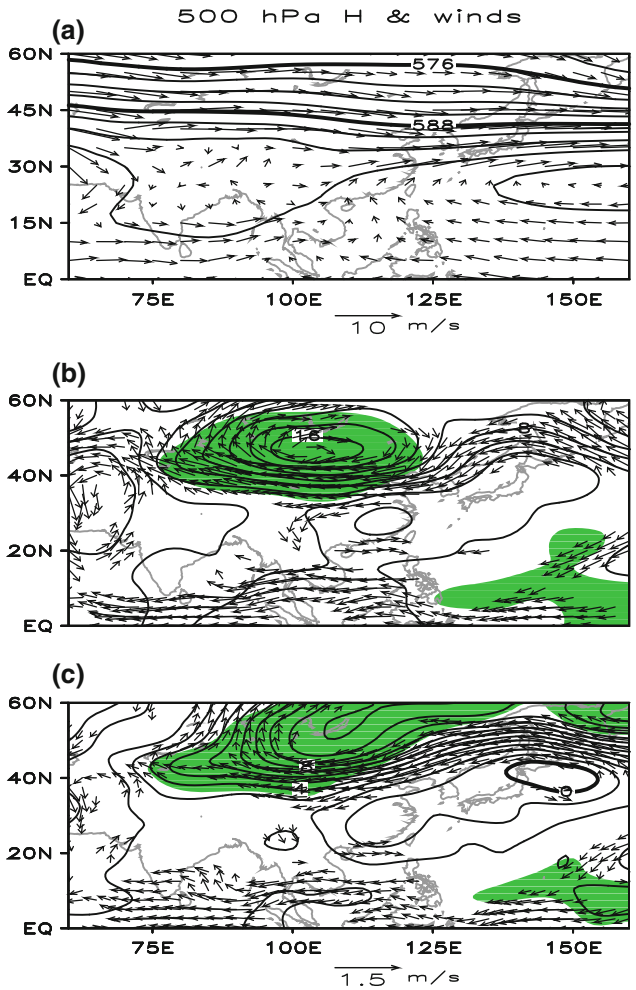

Fig. 5 Same as Fig. 4, but for the 500 hPa geopotential height (H500) and winds

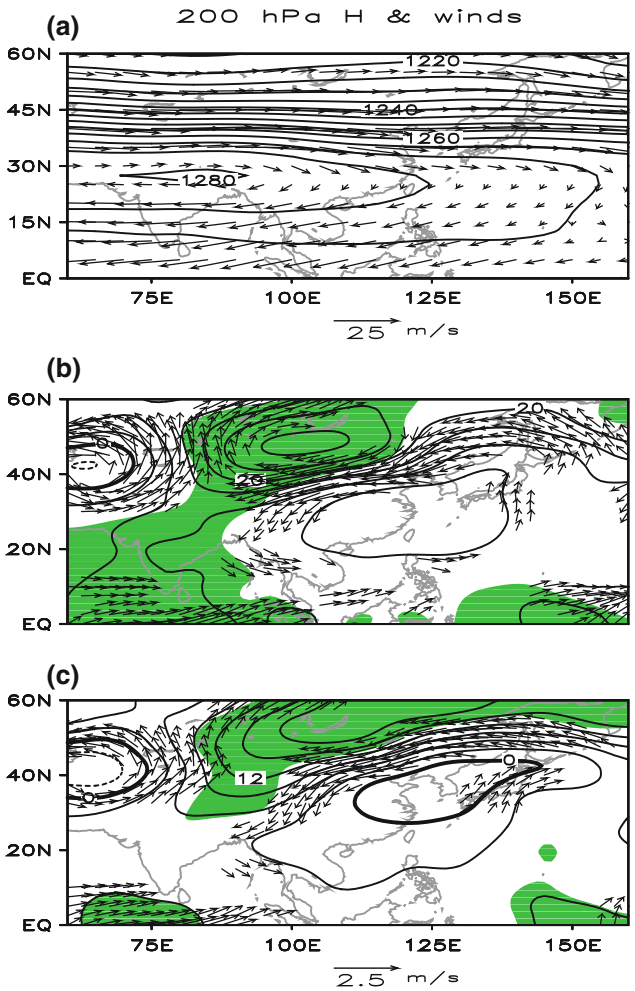

Fig. 6 The same as Fig. 4, but for the 200 hPa geopotential height (H200) and winds

fields. The results are shown in Fig. 8. The absolute values of the regressed H200 anomalies over northern China continuously increase from 1-month lead through 1-month lag. In 1-month lead (Fig. 8a), before more heatwaves take place, positive H200 anomalies emerge over northern China, favoring the high pressure anomalies over Mongolia and the adjacent regions. From 0-month lead through 1-month lag (Fig. 8b, c), the high pressure anomalies are enhanced, which indicates that the northern China mode has a positive feedback to the GHAs over Mongolia and the adjacent regions. Thus, the northern China mode of the HWF may be at least in part due to such positive feedback with the GHAs over Mongolia and the adjacent regions.

To further clarify the physical processes of the GHAs over Mongolia and the adjacent regions impacting on the heatwaves, Fig. 9 presents the TCC anomalies lead-lag regressed to PC1(ID). In corresponding to a positive phase of the northern China mode, the reduced TCC anomalies over northern China persist from 1-month lead through 1-month lag, reaching maximum during the simultaneous period. Figure 10 shows the SSR anomalies lead-lag regressed to PC1(ID). Associated with a positive phase of the northern China mode, the increased net shortwave radiation at the surface can be observed over northern China and sustain from 1-month lead through 1-month lag.

In light of these, the possible physical processes might be summarized as following. The reduced TPSC may induce high pressure anomalies at mid- and upper troposphere over Mongolia and the adjacent regions The subsidence associated with the high pressure anomalies tends to suppress the local cloud formation, which increases the net radiation budget, heats the surface, and favors more heatwaves (see Fig. 1 in Alexander 2010). On the other hand, the local surface heating can excite the high pressure anomalies at mid- and upper troposphere and further strengthens the local high pressure system. Through such positive feedback effect, the TPSC anomaly is tied to the anomalous HWF over northern China. Note that the reason why the TCC and the SSR are introduced to interpret the relevant physical process is based on the research result by Alexander (2010)

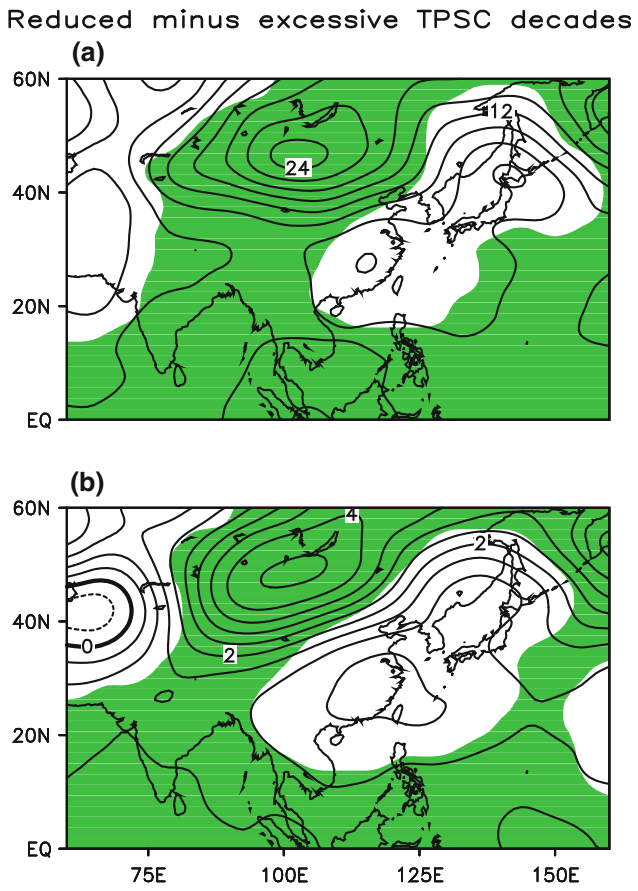

Fig. 7 Composite difference of JJA **a** H500 and **b** H200 (contours in units of 10 gpm) between the reduced and excessive TPSC decades (reduced minus excessive). The *shadings* denote anomalies exceeding 95 % significance level based on the Student's *t* test

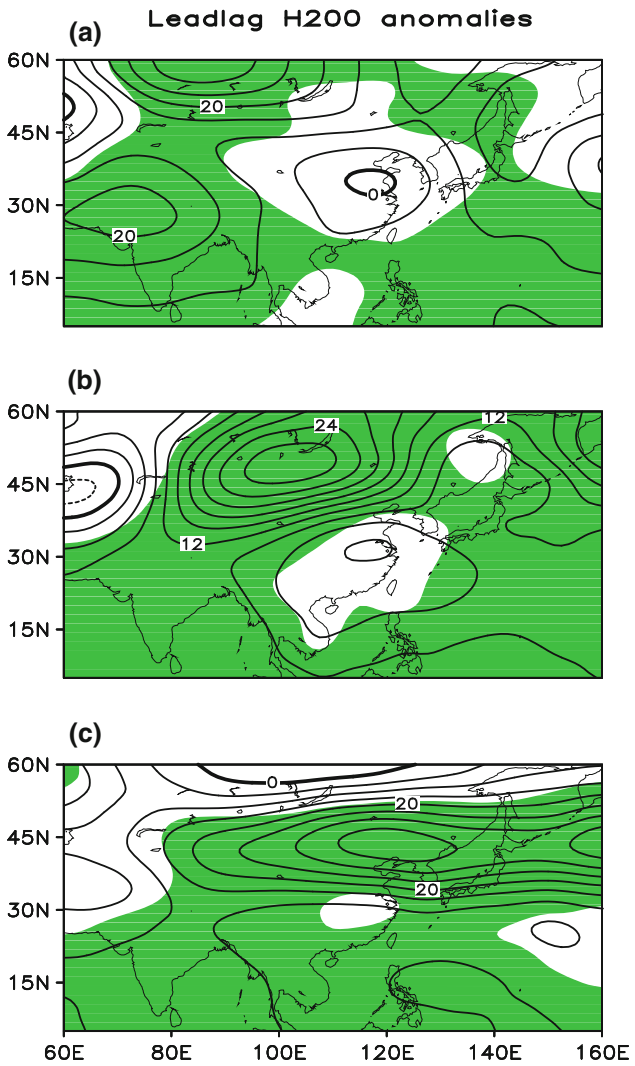

Fig. 8 The lead-lag H200 anomalies regressed to PC1(ID) (contours in units of gpm). PC1(ID) leads the H200 by **a** −1 **b** 0, and **c** 1 month. Note that −1, 0, and 1 month correspond to May, JJA and September, respectively. *Color shadings* denote the 95 % confidence level based on the Student's *t* test

and Hirschi et al. (2010). They found that cloud cover and net shortwave radiation near the surface play critical roles in the heatwave formation in dry regions.

To elucidate the effects of an anomalous TPSC forcing on the GHAs at mid- and upper levels over northern China, we performed a numerical experiment with the non-linearized SGCM to see what effects changing the TPSC will have on planetary-scale atmospheric circulations. The existence of the anomalous snow cover works to cut the upward sensible heat flux rather than the evaporation over TP because of its dry ground condition (Ose 1996). To mimic the diabatic heating of the reduced TPSC, we imposed a warming anomaly centered at 75°E, 35°N which has an elliptical squared cosine distribution in latitude and longitude with a maximum heating being 2.5 K/day near 500 hPa (Wu et al. 2012). The perturbed experiments were integrated for 3,700 days. The last 3600-day integrations were used to construct an ensemble (arithmetic) mean. Note that the result is not sensitive to the selection of initial condition, since the analysis is conducted for the period after the climate equilibrium is reached.

The model responses of 250 hPa geopotential height (H250) to the reduced TPSC forcing are shown in Fig. 11a. A high anomaly is induced at upper troposphere and centered over northern China. The 550 hPa geopotential height (H550) exhibits a similar pattern with H250 (Fig. 11b). At the lower level (950 hPa), air temperatures respond a warm center over northern China which extends eastward to the North Pacific and southwestward towards TP (Fig. 11c). The numerical experiment confirms that the anomalous TPSC forcing can excite high pressure anomalies at the middle and upper troposphere and warm anomalies at the lower level over northern China. Note that the simulation has some discrepancies in the middle latitudes north of 45°N (the position of the geopotential height negative center in particular) or central Asia, if compared with

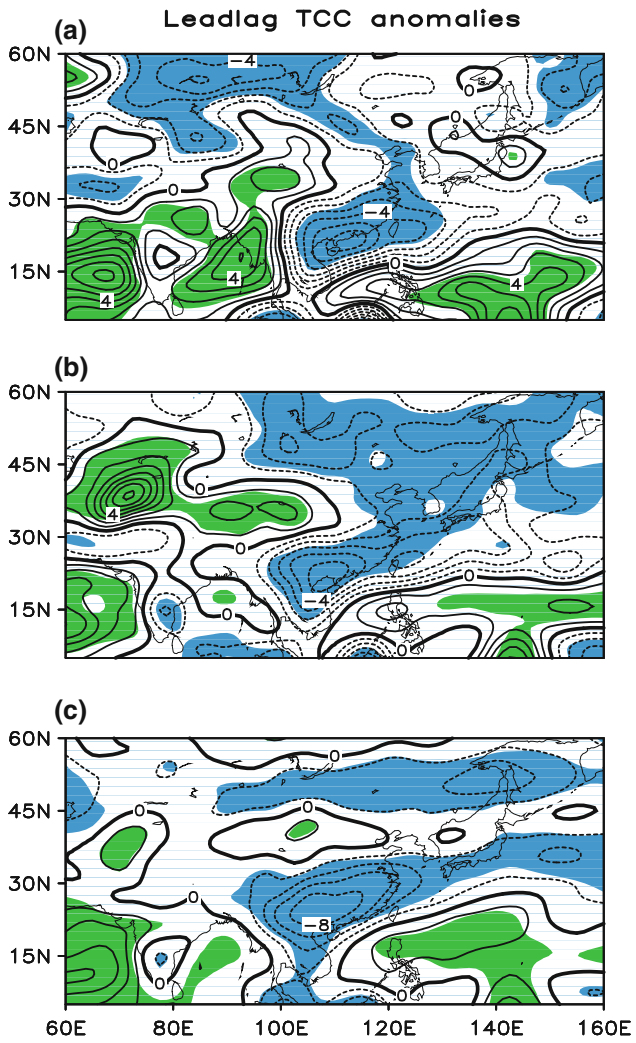

Fig. 9 Same as Fig. 8, but for the total cloud cover (TCC; in unit of %)

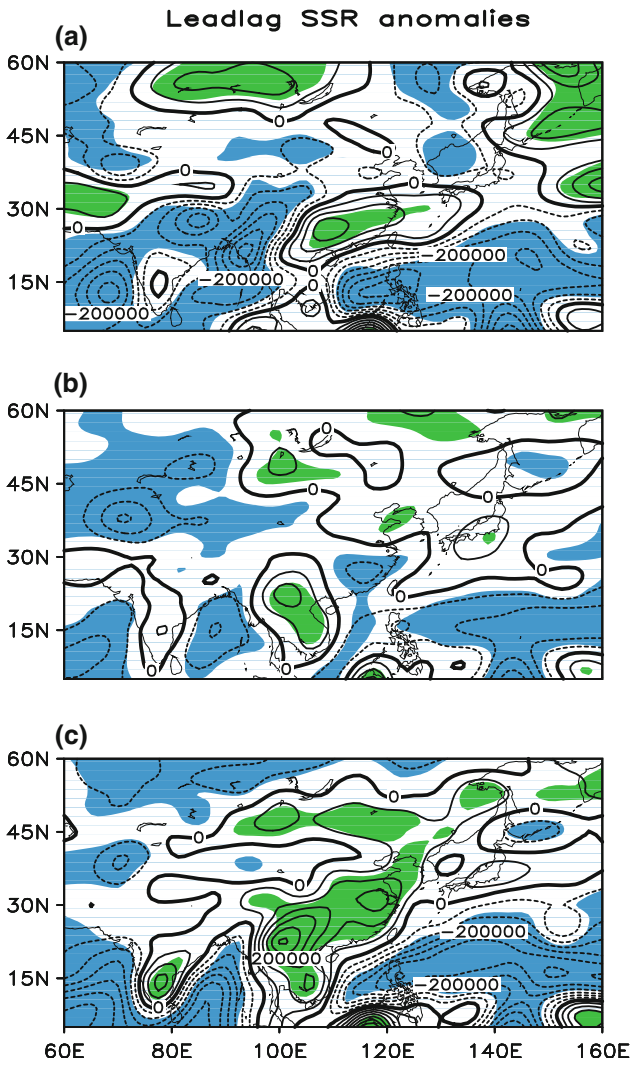

Fig. 10 Same as Fig. 8, but for the surface solar radiation (SSR; in unit of W m^{-2} s). The interval of contours is 50,000 W m^{-2} s

Fig. 6b. It implies that the TPSC anomaly cannot well interpret the circulation variations over these regions and some other factors may dominate the circulations there.

The following presents the theoretical evidence that the primary response of the high pressure anomalies over Mongolia and the adjacent regions to the reduced TPSC is the southwestward tilt towards TP as observed in Sect. 3. According to Li et al. (2010), for the TPSC forcing, the slope of the high ridge axis, $k(k_x, k_y)$, meets the following relationship:

$$k_x \equiv \left(\frac{\partial x}{\partial z}\right) = -\frac{1}{T}\left(\frac{\partial T}{\partial x}\right)_p \Big/ \left(\frac{\partial^2 z}{\partial x^2}\right)_p \quad (1)$$

$$k_y \equiv \left(\frac{\partial y}{\partial z}\right) = -\frac{1}{T}\left(\frac{\partial T}{\partial y}\right)_p \Big/ \left(\frac{\partial^2 z}{\partial y^2}\right)_p . \quad (2)$$

According to Formulas (1) and (2), for the high ridge axis, $\left(\frac{\partial^2 z}{\partial x^2}\right)_p < 0$, $\left(\frac{\partial^2 z}{\partial y^2}\right)_p < 0$, the axis tilts to the warm side. Therefore, under the reduced TPSC forcing, the axis of the high pressure anomalies over Mongolia and the adjacent regions tends to tilt southwestward towards the warming TP.

To summarize, the primary response of the atmosphere to the reduced TPSC is a high pressure anomaly at mid- and upper troposphere over Mongolia and the adjacent regions which tilts southwestward towards TP. Such high pressure anomalies favor more heatwaves in northern China via triggering the positive feedback among the H, TCC and surface heating.

5 Conclusion and discussion

Climate change is expected to affect not only the means of climatic variables, but also their variabilities and extremes such as heatwaves (e.g., Easterling et al. 2000; Wu et al. 2006, 2010). In this study, we examined the observed relationship between the TPSC and the HWF across China and

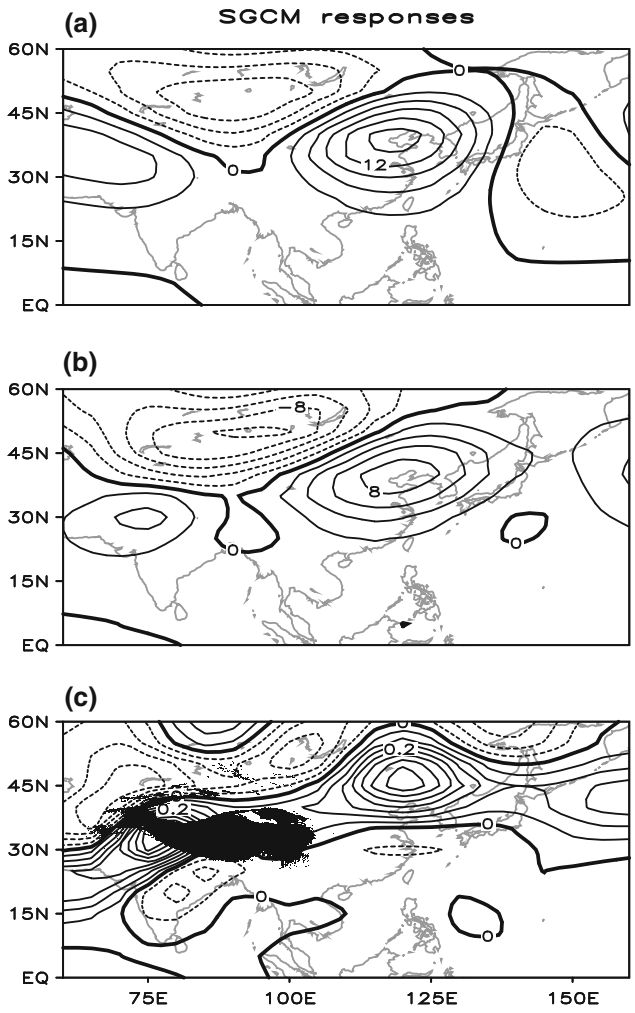

Fig. 11 JJA **a** 250 hPa geopotential height (H250), **b** 550 hPa geopotential height (H550) (in units of gpm), and 950 hPa temperature (T950) (in units of K) responses to the reduced TPSC forcing in the SGCM

found that the decadal to interdecadal variations of northern China HWF are significantly connected with the TPSC. A reduced TPSC is often accompanied by more heatwaves over northern China, and vice versa. Numerical experiments suggest that the anomalous TPSC can induce a high pressure anomaly over northern China which in turn modifies the local cloud formation, the net radiation budget, and the HWF. On the other hand, the HWF responds a positive feedback to the anomalous geopotential height at mid- and upper troposphere over Mongolia and the adjacent regions. Through such physical processes, the TPSC is linked to the northern China HWF. Since the TPSC is expected to further decrease with increasing levels of greenhouse gases in the atmosphere in future (Meehl et al. 2007), the results obtained in this study imply that the TPSC may play an increasingly important role in shaping northern China heatwaves in next decades.

Besides the above positive feedback process, it should be pointed out that some negative feedbacks also modulate the HWF decadal-to-interdecadal variability. For example, the EOF2 mode has considerably amplified since mid-1990s, but with the opposite polarity to the EOF1 mode (particularly over northeastern China) (Fig. 2). The resemblance between the EOF2 mode and the China summer precipitation anomaly pattern implies that the intensified precipitation may reduce the local HWF (northeastern China in particular). As a matter of fact, Zhao et al. (2010) suggested that the thermal state of TP may alter the East Asian thermal contrast and summer monsoon rainfall. In addition, other factors (including the remote oceanic impacts and greenhouse gas concentrations) can also affect the northern China HWF (e.g., Hu et al. 2003; Ding et al. 2008, 2009; Meehl et al. 2009; Alexander 2010).

The decadal to interdecadal variations of the northern China HWF revealed in this study may be a part of China summer climate shift around 1996–1998. One of the biggest problems is lack of access to high-quality, long-term climate data in investigating the decadal to interdecadal changes in extreme weather and climate events such as heatwaves (Easterling et al. 2000). For instance, the TPSC data in this study is available only from 1968. Due to the limitation of data time length, it is difficult to obtain unequivocal evidence of climate change. Therefore, monitoring efforts should receive enhanced support.

Acknowledgments We appreciate the National Meteorological Information Center of China for providing the gauge station data across China and the Global Snow Lab (Rutgers University) for the snow cover extent area data and the three anonymous reviewers for their helpful comments and suggestions. This work is supported by the National Basic Research Program "973" (Grant No. 2010CB950400), a project funded by the Priority Academic Program Development of Jiangsu Higher Education Institutions (PAPD), and the Special Research Program for Public Welfare (Meteorology) of China (Grant Nos. GYHY200906016 and GYHY201006020).

References

Alexander L (2010) Extreme heat rooted in dry soils. Nat Geosci 3:1–2

Ding YH (1992) Summer monsoon rainfalls in China. J Meteorol Soc Jpn 70:397–421

Ding YH, Ren GY, Zhao ZC, Xu Y, Luo Y, Li QP, Zhang J (2007) Detection, causes and projection of climate change over China: an overview of recent progresses. Adv Atmos Sci 24(6):954–971

Ding YH, Wang ZY, Sun Y (2008) Inter-decadal variation of the summer precipitation in East China and its association with decreasing Asian summer monsoon. Part I: observed evidences. Inter J Climatol 28(9):1139–1161

Ding YH, Sun Y, Wang ZY, Zhu YX, Song YF (2009) Inter-decadal variation of the summer precipitation in East China and its association with decreasing Asian summer monsoon. II: possible causes. Inter J Climatol 29(13):1926–1944

Duan AM, Li F, Wang MR, Wu GX (2011) Persistent weakening trend in the spring sensible heat source over the Tibetan Plateau and its impact on the Asian summer monsoon. J Climate 24: 5671–5682

Easterling DR, Evans JL, Groisman PY, Karl TR, Kunkel KE, Ambenje P (2000) Observed variability and trends in extreme climate events: a brief review. Bull Am Meteor Soc 81:417–425

Fischer EM, Schär C (2010) Consistent geographical patterns of changes in high-impact European heatwaves. Nat Geosci 3:398–403

Fu CB (2003) Potential impacts of human-induced land cover change on East Asia monsoon. Global Planet Change 37:219–229

Garcia-Herrera R, Diaz J, Trigo RM, Luterbacher J, Fischer EM (2010) A review of the European summer heatwave of 2003. Crit Rev Environ Sci Technol 40:267–306

Hall NMJ (2000) A simple GCM based on dry dynamics and constant forcing. J Atmos Sci 57:1557–1572

Hirschi M, Seneviratne SI, Alexandrov V, Boberg F, Boroneant C, Christensen OB, Formayer H, Orlowsky B, Stepanek P (2010) Observational evidence for soil-moisture impact on hot extremes in southeastern Europe. Nat Geosci 3. doi:10.1038/NGEO1032

Hu ZZ (1997) Interdecadal variability of summer climate over East Asia and its association with 500 hPa height and global sea surface temperature. J Geophys Res 102(D16):19403–19412

Hu ZZ, Yang S, Wu R (2003) Long-term climate variations in China and global warming signals. J Geophys Res 108(19):4614. doi:10.1029/2003JD003651

Kalnay E, Kanamitus M, Kistler R et al (1996) The NCEP/NCAR 40-year reanalysis project. Bull Am Meteor Soc 77:437–471

Li J, Yu RC, Zhou TJ, Wang B (2005) Why is there an early spring cooling shift downstream of the Tibetan Plateau? J Clim 18:4660–4668

Li JP, Wu ZW, Jiang ZH, He JH (2010) Can global warming strengthen the East Asian summer monsoon? J Clim 23:6696–6705

Liu J, Chen R (2011) Studying the spatiotemporal variation of snow-covered days over China based on combined use of MODIS snow-covered days and in situ observations. Theo Appl Climatol. doi:10.1007/s00704-011-0441-9

Massimo B, Benedict S (2004) The role of the Himalayas and the Tibetan Plateau within the Asian monsoon system. Bull Amer Meteor Soc 85:1001–1004

Meehl GA et al (2007) Global climate projections. In: Solomon S et al (eds) Climate change 2007: the physical science basis: fourth assessment report of the intergovernmental panel on climate change. Cambridge University Press, Cambridge

Meehl GA et al (2009) Decadal prediction. Bull Am Meteor Soc 90:1467–1485

Nitta T, Hu ZZ (1996) Summer climate variability in China and its association with 500 hPa height and tropical convection. J Meteorol Soc Jpn 74(4):425–445

North GR, Bell TL, Cahalan RF, Moeng FJ (1982) Sampling errors in the estimation of empirical orthogonal functions. Mon Wea Rev 110:699–706

Ose T (1996) The comparison of the simulated response to the regional snow mass anomalies over Tibet, eastern Europe, and Siberia. J Meteorol Soc Jpn 74:845–866

Pu ZX, Xu L, Salomonson VV (2007) MODIS/Terra observed seasonal variations of snow cover over the Tibetan Plateau. Geophys Res Lett 34:L06706. doi:10.1029/2007GL029262

Qian YF, Zheng YQ, Zhang Y, Miao MQ (2003) Responses of China's summer monsoon climate to snow anomaly over the Tibetan Plateau. Inter J Climatol 23(6):593–613

Seol KH, Hong SY (2009) Relationship between the Tibetan Snow in spring and the East Asian summer monsoon in 2003: a global and regional modeling study. J Clim 22:2095–2110

Sutton RT, Hodson D (2005) Atlantic Ocean forcing of North American and European summer climate science. Science 309:115–118

Trenberth KE, Jones PD, Ambenje P, Bojariu R, Easterling D, Klein Tank A, Parker D, Rahimzadeh F, Renwick JA, Rusticucci M, Soden B, Zhai P (2007) Observations: surface and atmospheric climate change. In: Solomon S, Qin D, Manning M, Chen Z, Marquis M, Averyt KB, Tignor M, Miller HL (eds) Climate change 2007: the physical science basis. Contribution of working group 1 to the fourth assessment report of the intergovernmental panel on climate change. Cambridge University Press, Cambridge

Uppala SM, Kallberg PW, Simmons AJ, Andrae U, da Costa Bechtold V, Fiorino M, Gibson JK, Haseler J, Hernandez A, Kelly GA, Li X, Onogi K, Saarinen S, Sokka N, Allan RP, Andersson E, Arpe K, Balmaseda MA, Beljaars ACM, van de Berg L, Bidlot J, Bormann N, Caires S, Chevallier F, Dethof A, Dragosavac M, Fisher M, Fuentes M, Hagemann S, Hólm E, Hoskins BJ, Isaksen L, Janssen PAEM, Jenne R, McNally AP, Mahfouf JF, Morcrette JJ, Rayner NA, Saunders RW, Simon P, Sterl A, Trenberth KE, Untch A, Vasiljevic D, Viterbo P, Woollen J (2005) The ERA-40 re-analysis. Quart J Roy Meteor Soc 131:2961–3012

Wang B, Ding Q (2006) Changes in global monsoon precipitation over the past 56 years. Geophys Res Lett 33:L06711. doi:10.1029/2005GL025347

Wang B, Bao Q, Hoskins B, Wu G, Liu Y (2008a) Tibetan Plateau warming and precipitation change in East Asia. Geophys Res Lett 35:L14702. doi:10.1029/2008GL034330

Wang B, Wu ZW, Li JP, Liu J, Chang CP, Ding YH, Wu GX (2008b) How to measure the strength of the East Asian summer monsoon. J Clim 17:4449–4462

Wang B, Wu ZW, Chang CP, Liu J, Li JP, Zhou TJ (2010) Another look at interannual to interdecadal variations of the East Asian winter monsoon. J Clim 23:1495–1512

Wu R, Kirtman BP (2007) Observed relationship of spring and summer East Asian rainfall with winter and spring Eurasian snow. J Clim 20:1285–1304

Wu ZW, Li JP, He JH, Jiang ZH (2006) Occurrence of droughts and floods during the normal monsoons in the mid- and lower reaches of the Yangtze River. Geophys Res Lett 33:L05813. doi:10.1029/2005GL024487

Wu GX et al (2007) The Influence of mechanical and thermal forcing by the Tibetan Plateau on Asian climate. J Hydrometeor 8:770–789

Wu ZW, Wang B, Li JP, Jin FF (2009) An empirical seasonal prediction model of the East Asian summer monsoon using ENSO and NAO. J Geophys Res 114:D18120. doi:10.1029/2009JD011733

Wu R, Wen ZP, Yang S, Li YQ (2010) An interdecadal change in southern China summer rainfall around 1992–1993. J Clim 23:2389–2403

Wu ZW, Li JP, Jiang ZH, Ma TT (2012) Modulation of the Tibetan Plateau snow cover on the ENSO teleconnections: from the East Asian summer monsoon perspective. J Clim 25:2481–2489. doi:10.1175/JCLI-D-11-00135.1

Yu RC, Wang B, Zhou TJ (2004) Climate effects of the deep continental stratus clouds generated by the Tibetan Plateau. J Clim 17:2702–2713

Zhai PM, Sun AJ, Ren FM, Liu XN, Gao B, Zhang Q (1999) Changes of climate extremes in China. Clim Change 42:203–218

Zhang Y, Li T, Wang B (2004) Decadal change of the spring snow depth over the Tibetan Plateau: the associated circulation and influence on the East Asian summer monsoon. J Clim 17:2780–2793

Zhao P, Zhou ZJ, Liu JP (2007) Variability of Tibetan spring snow and its associations with the hemispheric extratropical circulation and East Asian summer monsoon rainfall: an observational investigation. J Clim 20:3942–3955

Zhao P, Yang S, Yu RC (2010) Long-term changes in rainfall over eastern China and large-scale atmospheric circulation associated with recent global warming. J Clim 23:1544–1562

Zhu XY, He JH, Wu ZW (2007) Meridional seesaw-like distribution of the Meiyu rainfall over the Changjiang-Huaihe River Valley and characteristics in the anomalous climate years. Chin Sci Bull 52(17):2420–2428